However, ketamine, pentobarbital and ODT have inhibitory effects. The mechanisms of inhibition by intravenous anesthetics are different from those of volatile anesthetics.

Metabotropic glutamate receptors

The metabotropic glutamate receptors (mGluRs) are distinct from the other metabotropic receptors in that they are much larger proteins and show little sequence similarity to most members of the GPCR family, although there is appreciable homology with the γ-aminobutyric acid B (GABA$_B$) receptors [48]. The mGluRs are important modulators of synaptic transmission in the mammalian CNS, and are believed to play roles in memory and learning. Therefore, it was of interest to determine whether anesthetics and analgesics affect the function of these receptors. The mGluRs form a family of receptors with eight different subtypes (mGluR1-8 [49, 50]). Based on their pharmacology, second messenger coupling, and sequence differences, these receptors can be divided into Classes I (mGluR1 and mGluR5), II (mGluR2 and mGluR3), and III (mGluR4 and mGluR6-8) [51]. The Class I receptors are linked to learning and memory [51] in pharmacological studies showing that an agonist of mGluR1 and mGluR5 enhances memory and that mutant mice lacking mGluR1 show deficits in learning and memory and reduced hippocampal LTP [51–53]. Mice lacking mGluR1 also display poor motor coordination. More recently, it was reported that mice lacking mGluR5 show impaired learning and reduced CA1 LTP, but normal CA3 LTP [54]. In view of the effects of ethanol and anesthetics on learning, memory, and motor function, it is of interest to consider the effects of these drugs on Class I mGluRs.

There are few studies of the effects of anesthetic agents on mGluRs. Ethanol inhibits quisqualate-induced burst activity in rat cultured cerebellar Purkinje neurons, which are mediated by mGluRs [55], and quisqualate-induced currents in Xenopus oocytes expressing mRNA from rat cerebellum [56], but does not affect the glutamate-stimulated phospholipase C activity of brain astrocytes [57]. These results suggest that ethanol inhibits some, but not all, mGluR subtypes, and encouraged us to test the effects of ethanol and anesthetics on specific mGluR subtypes expressed in Xenopus oocytes.

The effects of ethanol and halothane, on the function of mGluR1 and mGluR5 expressed in Xenopus oocytes have been reported [8]. Halothane and ethanol inhibited mGluR5-induced Ca^{2+}-activated Cl^- currents, yet pharmacologically relevant concentrations of these compounds had little effect on the glutamate-induced currents in the oocytes expressing mGluR1. The GF109203X abolished the inhibitory effects of halothane and ethanol on

mGluR5s. Conversely, the phosphatase inhibitor calyculin A prolonged the actions of halothane and ethanol. Furthermore, mutation of a PKC consensus site (Ser890) of mGluR5 abolished the inhibitory effects of halothane and ethanol. These results suggest that ethanol and volatile anesthetics inhibit mGluR5 because they promote PKC-mediated phosphorylation.

Orexin A receptor

Neurons in the hypothalamus containing the neuropeptide orexin have been implicated in the control of sleep and wakefulness and in the pathology of narcolepsy. We have investigated the effects of volatile anesthetics, ethanol and intravenous anesthetics on orexin-A-induced Ca^{2+}-activated Cl^- currents using Xenopus oocytes expressing orexin-1 receptors (OX1Rs) [58]. The volatile anesthetics isoflurane, enflurane and halothane inhibited Cl^- currents elicited by 1-micromol/l orexin-A. Pentobarbital and ketamine also inhibited the action of orexin-A. Dexmedetomidine had little inhibition on the orexin A-induced current in oocytes expressing the OX1Rs [26]. Although more study would be necessary, these results may, at least in part, explain the hypnotic effects of these anesthetics.

The effect of anesthetics and analgesics on G$_i$ protein coupled receptors

The targets of anesthetics and analgesics are not only G$_q$ coupled receptors; other GPCRs can be targets as well. There has been little information regarding G$_s$- and G$_i$-coupled receptors, especially. Especially, the G$_i$ coupled receptors, have been thought of as one of the sites of the anesthetics and analgesics. However, historically there have not been convenient assay systems to study the effects of anesthetics and analgesics on G$_i$ coupled receptors. Because stimulation of G$_i$ coupled receptors results in inhibition of cyclic AMP in cells and dose does not affect the Ca^{2+} elevation; the system has been well characterized, and has proven useful for studying the effects of intravenous anesthetics on GPCRs.

Recently, several investigators reported assay systems using chimera G proteins between G$_i$ and G$_q$ for investigation of G$_i$ coupled receptors (Table 4). Coward et al. [59], have reported that the chimeric G proteins alter

Table 4 The effects of anesthetics on Gi coupled receptor function

	Halothane	Sevoflurane	Ketamine	Propofol
M$_2$	↓			
μ opioid	↓	↓	↓	→
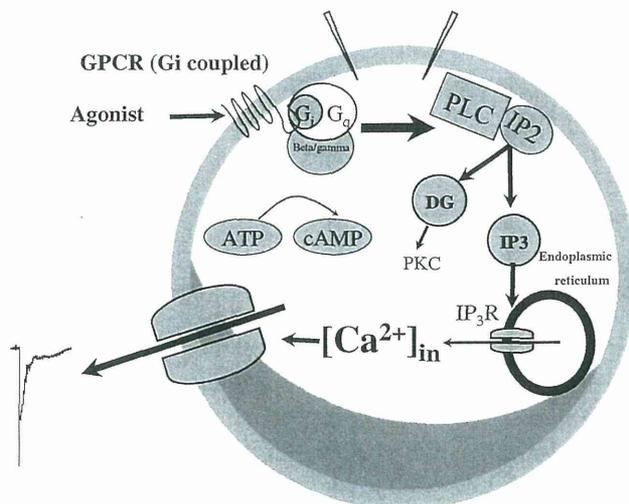
Fig. 3 Intracellular signaling in *Xenopus* oocytes expressing a Gi coupled receptor fused to chimeric Gα protein Gq$_{i5}$. Stimulation of G$_{i/o}$ coupled receptor fused to Gq$_{i5}$ leads to Gq$_{i5}$ protein-dependent activation of phospholipase C, resulting in the formation of IP$_3$ and diacylglycerol. The IP$_3$ causes the release of Ca^{2+} from the endoplasmic reticulum, which in turn triggers the opening of Ca^{2+}-activated Cl$^-$ channels in *Xenopus* oocytes

receptor coupling so that signaling can occur through G$_q$ and result in mobilization of intracellular calcium stores in CHO cells. From this evidence, we drew a hypothesis that it may be able to used for the analysis by injecting both cRNA the G$_{i/q}$ chimaeric G proteins (G$_{i/q}$) and M2R into the *Xenopus* oocytes as well as G$_q$ coupled receptors. To establish the system, we investigated whether we could measure if the acetylcholine stimulation leads to activation of phospholipase C, resulting in the formation of IP$_3$ and diacylglycerol and the release of Ca^{2+} from the endoplasmic reticulum, which in turn triggers the opening of Ca^{2+}-activated Cl$^-$ channels in *Xenopus* oocytes which were injected both cRNA and the G$_{i/q}$ chimera G proteins and G$_i$ coupled receptor, M2R [60] (Table 4). However, regarding the established analysis of injecting both cRNA the G$_{i/q}$ chimaeric G proteins and M2R into the *Xenopus* oocytes as well as G$_q$ coupled receptors, there were some problems for assay, i.e, low expression rates and low evoking currents. Recently, in order to improve the G$_{i/o}$-coupled receptor assay system, we made a G$_{i/o}$-coupled receptor fused to Gq$_{i5}$ (μOR-G$_{qi5}$) and expressed it in *Xenopus* oocytes [61, 62] (Fig. 3). By using this assay system, we examined the effects of anesthetics on the function of μOR (Table 4).

The effects of anesthetics and on M2R

We examined ACh-induced Ca^{2+}-activated Cl$^-$ currents in *Xenopus* oocytes coexpressing G$_i$-coupled M2R with the

chimeric Gα_{qi5} [60]. In oocytes coexpressing M2R and Gα_{qi5}, halothane inhibited M2R -induced Cl$^-$ currents in a concentration-dependent manner, suggesting that halothane inhibits M$_2$R-induced cellular responses at clinically relevant concentrations. Treatment with the PKC inhibitor GF109203X produced a 3.5-fold enhancement of the initial Cl$^-$ currents induced by ACh in oocytes expressing M2R and G$_{qi5}$. The rate of halothane-induced inhibition of Cl$^-$ currents elicited by ACh, however, was not changed in such oocytes pretreated with GF109203X. These findings suggest that halothane inhibits the M2R-induced signaling by acting at sites other than PKC activity.

The effects of anesthetics and analgesics on opioid receptors

Opioids are commonly used analgesics in clinical practice, however, the actual role of opioid receptors (OR) in anesthetic action have been unclear. It has been reported that OR antagonist naloxone does not affect the anesthetic potency of halothane in animals [63, 64]. Moreover, naloxone dose does not antagonize the analgesic effects of inhalation anesthetics [65]. On the other hand, Sarton et al. [66], reported that S(+) ketamine interacts with the μ-opioid system at supraspinal sites. In order to make clear the role of ORs in anesthetic action, it would be necessary to study the direct effects on OR functions.

The ORs belong to the GPCR family and three types of opioid receptors, μ, δ and κ, have been identified by molecular cloning [67]. Within three subtypes of these receptors, μORs are the major receptor to mediate the analgesic effects of opioids [67]. On the basis of second messenger signaling, μOR couple to the G$\alpha_{i/o}$ protein to cause inhibition of adenylate cyclase, inhibition of voltage-dependent Ca^{2+} channels or activation of G protein-coupled inwardly rectifying K$^+$ channels (GIRKs) [67]. Functions of G$_q$ coupled receptors have been reported to be modified by some anesthetics and analgesics [5, 68]; as far as the functions of G$_{i/o}$-coupled receptors including μOR are concerned, much less is known about the direct effects of anesthetics and analgesics.

We and others have previously used oocytes expressing GIRK channels for the analysis of the function of G$_{i/o}$ protein-coupled receptors such as μOR, 5HT$_{1A}$R, GABA$_B$R or cannabinoid CB$_1$ receptors [62, 69–71]; GIRKs has been demonstrated as being reporter channels for assay of the activity of G$_{i/o}$-coupled receptors [69]. However, recent reports have revealed that GIRKs are possible targets for several anesthetics including halothane [72, 73]. Also, GIRKs have been reported to be possible targets for alcohol [74]. In such situations, it should be taken into consideration that functions of either G$_{i/o}$-coupled receptors or GIRKs, or both, could be affected by

anesthetics if GIRKs are used as reporters [72–74]. Thus, we employed a μOR fused to G_{qi5} (μOR-G_{qi5}) in the *Xenopus* oocyte expression assay system. Accordingly, this system makes possible the study of the direct effects of anesthetics on μOR functions.

In our recent report, halothane, ketamine, propofol and ethanol themselves had no effects on μOR-G_{qi5} in oocytes expressing μOR-G_{qi5} [61]. In contrast, ketamine and ethanol inhibited the [D-Ala2,N-Me-Phe4,Gly5-ol] enkephalin (DAMGO)-induced Cl^- currents at clinically equivalent concentrations. Halothane and propofol only inhibited the DAMGO-induced Cl^- currents at higher but clinically used concentrations. These findings suggest that ketamine and ethanol inhibit the μOR function directly in clinical practice.

Sevoflurane is commonly used together with opioids in clinical practice. However, the effects of sevoflurane on μOR functions are still unclear. Our recent study reveals that the effects of sevoflurane on the μOR functions were analyzed by using *Xenopus* oocytes expressing a μOR fused to chimeric $G\alpha$ protein Gq_{i5} (μOR-Gq_{i5}) [75]. Sevoflurane inhibited the DAMGO-induced Cl^- currents at clinically used concentrations by PKC activation. These findings suggest that sevoflurane would inhibit the μOR function in clinical practice. The same as with sevoflurane, propofol has been commonly used together with opioids clinically. From the viewpoint of the effects of the opioid receptors function, propofol may be a better choice than sevoflurane.

Future directions

Several lines of study have shown that GPCRs are also targets for them. It has been reported that some anesthetics inhibit the functions of G_q-coupled receptors, such as M1R. Although GPCRs are the most numerous therapeutic targets known, the ligands for approximately two-thirds of these receptors remain unknown. The challenge in the postgenomic era is to evaluate the role of these orphan GPCRs (oGPCRs) in normal physiology and disease, and to develop new therapies based on this information. Many oGPCRs are expressed in the brain, suggesting the existence of unidentified neurotransmitters. Nearly 160 GPCRs have been identified based on their gene sequence and ability to interact with known endogenous ligands. However, an estimated 500–800 additional GPCRs have been classified as "orphan" receptors (oGPCRs) because their endogenous ligands have not yet been identified. Given that known GPCRs are targets for anesthetics and analgesics, these oGPCRs represent a rich group of receptor targets for them.

Previous reports show that anesthetics affect the function of GPCRs, and this suggests that some oGPCRs are the targets of anesthetics. Several oGPCRs involved in pain and nociception have been reported [76]. Majane and Yang [76] reported that neuropeptide FF (NPFF) modulated pain sensation and morphine analgesia under normal and pathological conditions, via both spinal and brain mechanisms [77]. It would be interesting to study the effects of anesthetics on oGPCRs, which modulate pain like NPFF. More information about orphan GPCRs might help to elucidate the role of GPCRs in the mechanisms of anesthetics and analgesics.

The G_s- and G_i-coupled receptors might also be targets for anesthetics. Compared with Gq coupled GPCRs, there has been less information which shows the effects of anesthetics on G_s- and G_i-coupled receptors. The new assay systems using chimeric G protein [61] could be helpful to study them and make a role to help clarify their mechanisms .

Conclusion

Until today, ligand-gated ion channels, such as GABA, have been believed to be the site of action of the anesthetic. The mechanisms of anesthetics on GPCRs has become more evident in recent years. The action of anesthetics on GPCRs could also play an important role for anesthetic mechanisms. In particular, the effect of anesthetics on Gq protein coupled receptors has become apparent. The effects of anesthetics on Gs and Gi protein-coupled receptors are expected to be studied more in the future. In addition, the effect of anesthetics on the orphan receptor is not clear in how it works. It would be interesting to make clear the effects of anesthetics on these receptors. More time and more research on the effects of anesthetics for GPCRs, could make clear the mechanism of action of anesthetic agents in vivo.

References

1. Franks NP, Lieb WR. Molecular and cellular mechanisms of general anaesthesia. Nature. 1994;367:607–14.
2. Harris RA, Mihic SJ, Dildy-Mayfield JE, Machu TK. Actions of anesthetics on ligand-gated ion channels: role of receptor subunit composition. FASEB J. 1995;9:1454–62.
3. Campagna JA, Miller KW, Forman SA. Mechanisms of actions of inhaled anesthetics. N Engl J Med. 2003;348:2110–24.
4. Bonin RP, Orser BA. GABA(A) receptor subtypes underlying general anesthesia. Pharmacol Biochem Behav. 2008;90:105–12.
5. Minami K, Uezono Y. G_q protein-coupled receptors as targets for anesthetics. Curr Pharm Des. 2006;12:1931–7.
6. Minami K, Vanderah TW, Minami M, Harris RA. Inhibitory effects of anesthetics and ethanol on muscarinic receptors expressed in *Xenopus* oocytes. Eur J Pharmacol. 1997;339:237–44.

7. Minami K, Minami M, Harris RA. Inhibition of 5-hydroxytryptamine type 2A receptor-induced currents by n-alcohols and anesthetics. J Pharmacol Exp Ther. 1997;281:1136–43.

8. Minami K, Gereau RW IV, Minami M, Heinemann SF, Harris RA. Effects of ethanol and anesthetics on type 1 and 5 metabotropic glutamate receptors expressed in Xenopus laevis oocytes. Mol Pharmacol. 1998;53:148–56.

9. Minami K, Shiraishi M, Uezono Y, Ueno S, Shigematsu A. The inhibitory effects of anesthetics and ethanol on substance P receptors expressed in Xenopus oocytes. Anesth Analg. 2002;94:79–83.

10. Caulfield MP. Muscarinic receptors—characterization, coupling and function. Pharmacol Ther. 1993;58:319–79.

11. Fibiger HC. Cholinergic mechanisms in learning, memory and dementia: a review of recent evidence. Trends Neurosci. 1991;14:220–3.

12. Durieux ME. Halothane inhibits signaling through m1 muscarinic receptors expressed in Xenopus oocytes. Anesthesiology. 1995;82:174–82.

13. Eglen RM, Choppin A, Dillon MP, Hegde S. Muscarinic receptor ligands and their therapeutic potential. Curr Opin Chem Biol. 1999;3:426–32.

14. Wess J, Blin N, Yun J, Schoneberg T, Liu J. Molecular aspects of muscarinic receptor assembly and function. Prog Brain Res. 1996;109:153–62.

15. Wess J. Molecular biology of muscarinic acetylcholine receptors. Crit Rev Neurobiol. 1996;10:69–99.

16. Levey AI, Kitt CA, Simonds WF, Price DL, Brann MR. Identification and localization of muscarinic acetylcholine receptor proteins in brain with subtype-specific antibodies. J Neurosci. 1991;11:3218–26.

17. Anthony BL, Dennison RL, Aronstam RS. Disruption of muscarinic receptor-G protein coupling is a general property of liquid volatile anesthetics. Neurosci Lett. 1989;99:191–6.

18. Minami K, Yanagihara N, Toyohira Y, Tsutsui M, Shigematsu A, Wada A, Izumi F. Isoflurane inhibits nicotinic acetylcholine receptor-mediated $^{22}Na^+$ influx and muscarinic receptor-evoked cyclic GMP production in cultured bovine adrenal medullary cells. Naunyn Schmiedebergs Arch Pharmacol. 1994;349:223–9.

19. Lin LH, Leonard S, Harris RA. Enflurane inhibits the function of mouse and human brain phosphatidylinositol-linked acetylcholine and serotonin receptors expressed in Xenopus oocytes. Mol Pharmacol. 1993;43:941–8.

20. Nietgen GW, Honemann CW, Chan CK, Kamatchi GL, Durieux ME. Volatile anaesthetics have differential effects on recombinant m1 and m3 muscarinic acetylcholine receptor function. Br J Anaesth. 1998;81:569–77.

21. Do SH, Kamatchi GL, Durieux ME. The effects of isoflurane on native and chimeric muscarinic acetylcholine receptors: the role of protein kinase C. Anesth Analg. 2001;93:375–81.

22. Nietgen GW, Honemann CW, Durieux ME. Influence of anesthetics on endogenous and recombinantly expressed G protein-coupled receptors in the Xenopus oocyte. Toxicol Lett. 1998;100–101:319–27.

23. Durieux ME. Inhibition by ketamine of muscarinic acetylcholine receptor function. Anesth Analg. 1995;81:57–62.

24. Nagase Y, Kaibara M, Uezono Y, Izumi F, Sumikawa K, Taniyama K. Propofol inhibits muscarinic acetylcholine receptor-mediated signal transduction in Xenopus oocytes expressing the rat M1 receptor. Jpn J Pharmacol. 1999;79:319–25.

25. Shiraishi M, Minami K, Shibuya I, Uezono Y, Ogata J, Okamoto T, Murasaki O, Kaibara M, Ueta Y, Shigematsu A. The inhibitory effects of alphaxalone on M1 and M3 muscarinic receptors expressed in Xenopus oocytes. Anesth Analg. 2003;97:449–55.

26. Takizuka A, Minami K, Uezono Y, Horishita T, Yokoyama T, Shiraishi M, Sakurai T, Shigematsu A, Ueta Y. Dexmedetomidine inhibits muscarinic type 3 receptors expressed in Xenopus oocytes and muscarine-induced intracellular Ca^{2+} elevation in cultured rat dorsal root ganglia cells. Naunyn Schmiedebergs Arch Pharmacol. 2007;375:293–301.

27. Hollmann MW, Fischer LG, Byford AM, Durieux ME. Local anesthetic inhibition of m1 muscarinic acetylcholine signaling. Anesthesiology. 2000;93:497–509.

28. Hollmann MW, Wieczorek KS, Berger A, Durieux ME. Local anesthetic inhibition of G protein-coupled receptor signaling by interference with Gα(q) protein function. Mol Pharmacol. 2001;59:294–301.

29. Hollmann MW, Ritter CH, Henle P, de Klaver M, Kamatchi GL, Durieux ME. Inhibition of m3 muscarinic acetylcholine receptors by local anaesthetics. Br J Pharmacol. 2001;133:207–16.

30. Hollmann MW, Difazio CA, Durieux ME. Ca-signaling G-protein-coupled receptors: a new site of local anesthetic action? Reg Anesth Pain Med. 2001;26:565–71.

31. Frink MC, Hennies HH, Englberger W, Haurand M, Wilffert B. Influence of tramadol on neurotransmitter systems of the rat brain. Arzneimittelforschung. 1996;46:1029–36.

32. Shiraishi M, Minami K, Uezono Y, Yanagihara N, Shigematsu A. Inhibition by tramadol of muscarinic receptor-induced responses in cultured adrenal medullary cells and in Xenopus laevis oocytes expressing cloned M1 receptors. J Pharmacol Exp Ther. 2001;299:255–60.

33. Shiga Y, Minami K, Shiraishi M, Uezono Y, Murasaki O, Kaibara M, Shigematsu A. The inhibitory effects of tramadol on muscarinic receptor-induced responses in Xenopus oocytes expressing cloned M(3) receptors. Anesth Analg. 2002;95:1269–73.

34. Minami K, Ogata J, Horishita T, Shiraishi M, Okamoto T, Sata T, Shigematsu A. Intramuscular tramadol increases gastric pH during anesthesia. Can J Anaesth. 2004;51:545–8.

35. Nakamura M, Minami K, Uezono Y, Horishita T, Ogata J, Shiraishi M, Okamoto T, Terada T, Sata T. The effects of the tramadol metabolite O-desmethyl tramadol on muscarinic receptor-induced responses in Xenopus oocytes expressing cloned M1 or M3 receptors. Anesth Analg. 2005;101:180–6.

36. Eger EI 2nd, Zhang Y, Laster M, Flood P, Kendig JJ, Sonner JM. Acetylcholine receptors do not mediate the immobilization produced by inhaled anesthetics. Anesth Analg. 2002;94:1500–4.

37. Gyermek L. Pharmacology of serotonin as related to anesthesia. J Clin Anesth. 1996;8:402–25.

38. Kroeze WK, Kristiansen K, Roth BL. Molecular biology of serotonin receptors structure and function at the molecular level. Curr Top Med Chem. 2002;2:507–28.

39. Horishita T, Minami K, Uezono Y, Shiraishi M, Ogata J, Okamoto T, Shigematsu A. The tramadol metabolite, O-desmethyl tramadol, inhibits 5-hydroxytryptamine type 2C receptors expressed in Xenopus oocytes. Pharmacology. 2006;77:93–9.

40. De Koninck Y, Henry JL. Substance P-mediated slow excitatory postsynaptic potential elicited in dorsal horn neurons in vivo by noxious stimulation. Proc Natl Acad Sci USA. 1991;88:11344–8.

41. Xu XJ, Wiesenfeld-Hallin Z. Intrathecal neurokinin A facilitates the spinal nociceptive flexor reflex evoked by thermal and mechanical stimuli and synergistically interacts with substance P. Acta Physiol Scand. 1992;144:163–8.

42. Chapman V, Dickenson AH. The effect of intrathecal administration of RP67580, a potent neurokinin 1 antagonist on nociceptive transmission in the rat spinal cord. Neurosci Lett. 1993;157:149–52.

43. Cao YQ, Mantyh PW, Carlson EJ, Gillespie AM, Epstein CJ, Basbaum AI. Primary afferent tachykinins are required to experience moderate to intense pain. Nature. 1998;392:390–4.

44. Zimmer A, Zimmer AM, Baffi J, Usdin T, Reynolds K, König M, Palkovits M, Merey E. Hypoalgesia in mice with a targeted deletion of the tachykinin 1 gene. Proc Natl Acad Sci USA. 1998;95:2630–5.

45. De Felipe C, Herrero JF, O'Brien JA, Palmer JA, Doyle CA, Smith AJ, Laird JM, Belmonte C, Cervero F, Hunt SP. Altered nociception, analgesia and aggression in mice lacking the receptor for substance P. Nature. 1998;392:394–7.

46. Okamoto T, Minami K, Uezono Y, Ogata J, Shiraishi M, Shigematsu A, Ueta Y. The inhibitory effects of ketamine and pentobarbital on substance p receptors expressed in Xenopus oocytes. Anesth Analg. 2003;97:104–10.

47. Minami K, Yokoyama T, Ogata J, Uezono Y. The tramadol metabolite O-desmethyl tramadol inhibits substance P-receptor functions expressed in Xenopus oocytes. J Pharmacol Sci. 2011; 115:421–4.

48. Kaupmann K, Huggel K, Heid J, Flor PJ, Bischoff S, Mickel SJ, McMaster G, Angst C, Bittiger H, Froestl W, Bettler B. Expression cloning of GABA(B) receptors uncovers similarity to metabotropic glutamate receptors. Nature. 1997;386:239–46.

49. Abe T, Sugihara H, Nawa H, Shigemoto R, Mizuno N, Nakanishi S. Molecular characterization of a novel metabotropic glutamate receptor mGluR5 coupled to inositol phosphate/Ca^{2+} signal transduction. J Biol Chem. 1992;267:13361–8.

50. Conn PJ, Pin JP. Pharmacology and functions of metabotropic glutamate receptors. Annu Rev Pharmacol Toxicol. 1997;37: 205–37.

51. Riedel G. Function of metabotropic glutamate receptors in learning and memory. Trends Neurosci. 1996;19:219–24.

52. Aiba A, Chen C, Herrup K, Rosenmund C, Stevens CF, Tonegawa S. Reduced hippocampal long-term potentiation and context-specific deficit in associative learning in mGluR1 mutant mice. Cell. 1994;79:365–75.

53. Conquet F, Bashir ZI, Davies CH, Daniel H, Ferraguti F, Bordi F, Franz-Bacon K, Reggiani A, Matarese V, Condé F, Collingridge GL, Crépel F. Motor deficit and impairment of synaptic plasticity in mice lacking mGluR1. Nature. 1994;372:237–43.

54. Lu YM, Jia Z, Janus C, Henderson JT, Gerlai R, Wojtowicz JM, Roder JC. Mice lacking metabotropic glutamate receptor 5 show impaired learning and reduced CA1 long-term potentiation (LTP) but normal CA3 LTP. J Neurosci. 1997;17:5196–205.

55. Netzeband JG, Gruol DL. Modulatory effects of acute ethanol on metabotropic glutamate responses in cultured Purkinje neurons. Brain Res. 1995;688:105–13.

56. Sanna E, Dildy-Mayfield JE, Harris RA. Ethanol inhibits the function of 5-hydroxytryptamine type 1c and muscarinic M1 G protein-linked receptors in Xenopus oocytes expressing brain mRNA: role of protein kinase C. Mol Pharmacol. 1994;45: 1004–12.

57. Smith TL. Selective effects of ethanol exposure on metabotropic glutamate receptor and guanine nucleotide stimulated phospholipase C activity in primary cultures of astrocytes. Alcohol. 1994;11:405–9.

58. Minami K, Uezono Y, Sakurai T, Horishita T, Shiraishi M, Ueta Y. Effects of anesthetics on the function of orexin-1 receptors expressed in Xenopus oocytes. Pharmacology. 2007;79:236–42.

59. Coward P, Chan SD, Wada HG, Humphries GM, Conklin BR. Chimeric G proteins allow a high-throughput signaling assay of G_i-coupled receptors. Anal Biochem. 1999;270:242–8.

60. Minami K, Uezono Y, Shiraishi M, Okamoto T, Ogata J, Horishita T, Taniyama K, Shigematsu A. Analysis of the effects of halothane on G_i-coupled muscarinic M2 receptor signaling in Xenopus oocytes using a chimeric G alpha protein. Pharmacology. 2004;72:205–12.

61. Minami K, Sudo Y, Shiraishi S, Seo M, Uezono Y. Analysis of the effects of anesthetics and ethanol on μ-opioid receptor. J Pharmacol Sci. 2010;112:424–31.

62. Hojo M, Sudo Y, Ando Y, Minami K, Takada M, Matsubara T, Kanaide M, Taniyama K, Sumikawa K, Uezono Y. μ-Opioid receptor forms a functional heterodimer with cannabinoid CB_1 receptor: electrophysiological and FRET assay analysis. J Pharmacol Sci. 2008;108:308–19.

63. Harper MH, Winter PM, Johnson BH, Eger EI 2nd. Naloxone does not antagonize general anesthesia in the rat. Anesthesiology. 1978;49:3–5.

64. Pace NL, Wong KC. Failure of naloxone and naltrexone to antagonize halothane anesthesia in the dog. Anesth Analg. 1979;58:36–9.

65. Levine LL, Winter PM, Nemoto EM, Uram M, Lin MR. Naloxone does not antagonize the analgesic effects of inhalation anesthetics. Anesth Analg. 1986;65:330–2.

66. Sarton E, Teppema LJ, Olievier C, Nieuwenhuijs D, Matthes HW, Kieffer BL, Dahan A. The involvement of the mu-opioid receptor in ketamine-induced respiratory depression and antinociception. Anesth Analg. 2001;93:1495–500.

67. Surratt CK, Adams WR. G protein-coupled receptor structural motifs: relevance to the opioid receptors. Curr Top Med Chem. 2005;5:315–24.

68. Minami K, Uezono Y, Ueta Y. Pharmacological aspects of the effects of tramadol on G-protein coupled receptors. J Pharmacol Sci. 2007;103:253–60.

69. Dascal N. Signalling via the G protein-activated K+ channels. Cell Signal. 1997;9:551–73.

70. Uezono Y, Akihara M, Kaibara M, Kawano C, Shibuya I, Ueda Y, Yanagihara N, Toyohira Y, Yamashita H, Taniyama K, Izumi F. Activation of inwardly rectifying K^+ channels by GABA-B receptors expressed in Xenopus oocytes. NeuroReport. 1998;9: 583–7.

71. Ho BY, Uezono Y, Takada S, Takase I, Izumi F. Coupling of the expressed cannabinoid CB_1 and CB_2 receptors to phospholipase C and G protein-coupled inwardly rectifying K+ channels. Recept Channels. 1999;6:363–74.

72. Weigl LG, Schreibmayer W. G protein-gated inwardly rectifying potassium channels are targets for volatile anesthetics. Mol Pharmacol. 2001;60:282–9.

73. Yamakura T, Lewohl JM, Harris RA. Differential effects of general anesthetics on G protein-coupled inwardly rectifying and other potassium channels. Anesthesiology. 2001;95:144–53.

74. Lewohl JM, Wilson WR, Mayfield RD, Brozowski SJ, Morrisett RA, Harris RA. G-protein-coupled inwardly rectifying potassium channels are targets of alcohol action. Nat Neurosci. 1999;2:1084–90.

75. Minami K, Sudo Y, Yokoyama T, Ogata J, Takeuchi M, Uezono Y. Sevoflurane inhibits the μ-opioid receptor function expressed in Xenopus oocytes. Pharamacology. 2011;88:127–32.

76. Majane EA, Yang HY. Distribution and characterization of two putative endogenous opioid antagonist peptides in bovine brain. Peptides. 1987;8:657–62.

77. Panula P, Kalso E, Nieminen M, Kontinen VK, Brandt A, Pertovaara A. Neuropeptide FF and modulation of pain. Brain Res. 1999;848:191–6.
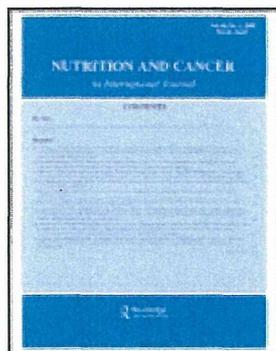
Nutrition and Cancer

Inhibitory Effects of Isoflavones on Tumor Growth and Cachexia in Newly Established Cachectic Mouse Models Carrying Human Stomach Cancers

Kazuyoshi Yanagihara [a] [b] , Misato Takigahira [c] , Keichiro Mihara [d] , Takanori Kubo [b] , Chie Morimoto [b] [e] , Yasuhiro Morita [b] , Kiyoshi Terawaki [f] , Yasuhito Uezono [f] & Toshio Seyama [b]

[a] Division of Genetics , National Cancer Center Research Institute , Tokyo , Japan

[b] Department of Life Sciences , Yasuda Women's University Faculty of Pharmacy , Hiroshima , Japan

[c] Investigative Treatment Division, Research Center for Innovative Oncology , National Cancer Center Hospital East , Chiba , Japan

[d] Department of Hematology/Oncology and Department of Cancer Research, Research Institute for Radiation Biology and Medicine , Hiroshima University , Hiroshima , Japan

[e] Department of Living Science Nutrition Course , Matsuyama Shinonome Junior College , Ehime , Japan

[f] Division of Cancer Pathophysiology, National Cancer Center Research Institute , Tokyo , Japan

PLEASE SCROLL DOWN FOR ARTICLE

Routledge
Taylor & Francis Group

Inhibitory Effects of Isoflavones on Tumor Growth and Cachexia in Newly Established Cachectic Mouse Models Carrying Human Stomach Cancers

Kazuyoshi Yanagihara

Division of Genetics, National Cancer Center Research Institute, Tokyo, Japan, and Department of Life Sciences, Yasuda Women's University Faculty of Pharmacy, Hiroshima, Japan

Misato Takigahira

Investigative Treatment Division, Research Center for Innovative Oncology, National Cancer Center Hospital East, Chiba, Japan

Keichiro Mihara

Department of Hematology/Oncology and Department of Cancer Research, Research Institute for Radiation Biology and Medicine, Hiroshima University, Hiroshima, Japan

Takanori Kubo

Department of Life Sciences, Yasuda Women's University Faculty of Pharmacy, Hiroshima, Japan

Chie Morimoto

Department of Life Sciences, Yasuda Women's University Faculty of Pharmacy, Hiroshima, Japan, and Department of Living Science Nutrition Course, Matsuyama Shinonome Junior College, Ehime, Japan

Yasuhiro Morita

Department of Life Sciences, Yasuda Women's University Faculty of Pharmacy, Hiroshima, Japan

Kiyoshi Terawaki and Yasuhito Uezono

Division of Cancer Pathophysiology, National Cancer Center Research Institute, Tokyo, Japan

Toshio Seyama

Department of Life Sciences, Yasuda Women's University Faculty of Pharmacy, Hiroshima, Japan

Cachexia, a negative prognostic factor, worsens a patient's quality of life. We established 2 novel cachexia models with the human stomach cancer cell line MKN-45, which was subcloned to produce potent cachexia-inducing cells by repeating the xenografts in immune-deficient mice. After subsequent xenografts, we isolated potent cachexia-inducing cells (MKN45cl85 and 85As2mLuc). Xenografts of MKN45cl85 cells in mice led to substantial weight loss and reduced adipose tissue and musculature volumes, whereas xenografts of 85As2mLuc cells resulted in highly metastatic and cachectic mice. Surgical removal of tumor tissues helped the mice regain body-weight in both mouse models. In vitro studies using these cells showed that isoflavones reduced their proliferation, implying that the isoflavones possess antiproliferative effects of these cancer cell lines. Isoflavone treatment on the models induced tumor cytostasis, attenuation of cachexia, and prolonged survival whereas discontinuation of the treatment resulted in progressive tumor growth and weight loss. The inhibitory effects of tumor growth and weight loss by isoflavones were graded as soy isoflavone aglycone AglyMax > daidzein > genistein. These results demonstrated that the 2 novel cachectic mouse models appear useful for analyzing the mechanism of cancer cachexia and monitoring the efficacy of anticachectic agents.

INTRODUCTION

Cancer cachexia, which is characterized by loss of musculature and fat tissue, anorexia, asthenia, and anemia, makes

therapeutic interventions less effective and is responsible for at least 20% of deaths in cancer patients (1–6). Recently, cachexia has been defined as a metabolic syndrome associated with underlying illness and physically characterized by loss of musculature, with or without loss of fat mass (2,3). One of its prominent clinical features is weight loss (adults) and growth failure (children). Anorexia, inflammation, insulin resistance, and increased muscle protein breakdown are frequently seen in patients with cachexia and are associated with increased morbidity (3). In cancer cachexia, weight loss is observed in 30% to 80% of patients, and in 15% the condition is very severe depending on the tumor types. Stomach or pancreatic cancer patients showed weight loss at very high frequencies, whereas in patients with non-Hodgkin's lymphoma, breast cancer, acute nonlymphocytic leukemia, or sarcomas, weight loss was less prominent (5,6). Cachexia is different from starvation, age-related loss of musculature, primary depression, malabsorption, and hyperthyroidism. Despite cachexia being a critical factor in clinical therapeutic treatments, the mechanisms causing cachexia have not been fully understood and there are only a few experimental studies on the mechanisms eliciting cachexia derived from stomach cancer (7,8).

Establishment of xenograft animal models is a promising way to investigate the pathological events of this devastating disorder. Xenograft mouse models of stomach cancer, which show human-like tumor progression and cachectic behavior, help to understand the disease and develop novel therapeutic approaches. Reports of cases of orthotopic implantation of stomach cancer cells into subserous regions of the stomach of host animals have shown that the subsequent tumor growth results in peritoneal dissemination and metastases to various organs/tissues, similar to human cases (9,10).

The isoflavones used in the present study were antioxidants (11). In addition, they have anticancer effects (12) and inhibit angiogenesis (13), topoisomerase (14), and tyrosine kinase (15). In the present study, we examined whether cachectic weight loss would be observed in 15 different stomach-cancer-bearing animals. Such loss, however, was observed with low frequency only in mice implanted with the MKN-45 cell line (16). From these mice, cachexia-inducing tumor cells were removed and cultured, and then cells were implanted into naïve mice. Cells inducing cancer cachexia steadily were isolated after 10 cycles of this stepwise selection (MKN45cl85 from MKN-45). Furthermore, orthotopic implantation of MKN45cl85 cells caused ascites formation in a few of the animals. We repeated cycles of isolation of ascetic tumor cells and orthotopic reimplantation of these cells into animals to isolate highly peritoneal metastatic cells. In the same way, the 85As2 cell line was established from MKN45cl85 cells in 11 cycles of stepwise selection. The 85As2mLuc cell line is highly metastatic and cachectic. Using these cachexia-inducing mouse models, we examined the biological effects of isoflavones (genistein, daidzein, and AglyMax) on potent cancer cells in vitro and in vivo. We have reported in an in vitro and in vivo study that isoflavones inhibit the growth

of several cell lines derived from human stomach cancer (17); however, these cancer cell lines are different from those newly established in this study. These 2 mouse models seem suitable for quantitative imaging studies of monitoring dynamic tumor growth as well as efficacy of anticachectic agents.

MATERIALS AND METHODS

Cell Lines and Culture

Twelve human stomach cancer cell lines (18), 10 human pancreatic cancer cell lines (19), and 5 malignant mesothelioma cell lines (20) had been established and used in our study (Table 1). Three stomach cancer cell lines (MKN-28, MKN-45, and MKN-72) were kindly provided by Dr T. Suzuki (Fukushima Medical University, Fukushima, Japan) (16). The MKN-45 cell line was established from gastric carcinoma of the poorly differentiated adenocarcinoma type from a freshly resected surgical specimen of the metastatic tumor of a 62-yr-old Japanese female patient. These cell lines were maintained in RPMI-1640 medium (GIBCO, Grand Island, NY) supplemented with 10% fetal bovine serum (FBS; GIBCO), 100 IU/mL penicillin G sodium, and 100 mg/mL streptomycin sulfate (GIBCO). All cell lines were routinely tested for Mycoplasma using a PCR Mycoplasma Detection kit (Takara, Kyoto, Japan), and no contamination was detected.

Cytokine Assay

The levels of secreted cytokines in culture supernatants or mouse sera were determined using an ELISA kit according to the manufacturer's instructions. Human interleukin (IL)-6, IL-10, transforming growth factor (TGF)-β, and tumor necrosis factor (TNF)-α assay kits were purchased from R&D Systems (Minneapolis, MN) and human TGF-α assay kit was purchased from Oncogene (Boston, MA). In brief, cells were seeded in 6-well plates (Nunc, Roskilde, Denmark) at 1×10^5 cells per well in RPMI-1640 medium containing 10% FBS. Following overnight incubation, the culture fluid was discarded and replaced by chemically defined medium composed of DMEM/Ham's F-12 (1:1) medium supplemented with 0.05% bovine serum albumin (21). Cell number and viability were monitored using the Trypan Blue exclusion method. Triplicate wells were harvested for 2 consecutive days and the culture supernatant was transferred to 96-well plates precoated with antibodies for the cytokine assay. The supernatant-antibody reactions were processed at room temperature for 2 h. After incubation, the plates were washed 3 times with washing buffer and immersed in a solution of secondary antibodies conjugated with horseradish peroxidase (HRP) for 2 h. A chromogen (tetramethylbenzidine) was then added for yielding reaction products with a specific wavelength absorbance. H_2SO_4 (1 M) was added to stop the reaction. The plates were read in a microplate reader (Wallac 1420 ARVO MX, Perkin Elmer, Waltham, MA).

TABLE 1
Cachexia-inducing cancer cell lines assessed by body weight loss

	Cell line	Tumor formation	Loss of body weight		Cell line	Tumor formation	Loss of body weight
Stomach	HSC-39	5/5	0/5	Pancreatic	Sui65	5/5	0/5
cancer	HSC-40A	5/5	0/5	cancer	Sui66	5/5	0/5
	HSC-41	5/5	0/5		Sui67	5/5	0/5
	HSC-42	5/5	0/5		Sui68	5/5	0/5
	HSC-43	5/5	0/5		Sui69	5/5	0/5
	HSC-44PE	5/5	0/5		Sui70	5/5	2/5
	HSC-45	5/5	0/5		Sui71	5/5	0/5
	HSC-57	5/5	0/5		Sui72	5/5	0/5
	HSC-58	5/5	0/5		Sui73	5/5	0/5
	HSC-59	5/5	0/5		Sui74	5/5	0/5
	HSC-60	5/5	0/5	Malignant mesothelioma	TCC-MESO-1	5/5	0/5
	HSC-64	5/5	0/5		TCC-MESO-3	5/5	0/5
	MKN-28	5/5	0/5		Me1Tu	5/5	0/5
	MKN-45	5/5	2/5		Me2Tu	5/5	0/5
	MKN-72	5/5	0/5		Me3Tu	5/5	0/5

Mice were implanted s.c. into left and right flank (1×10^6 cells suspended in 100 μL PBS /site). Four wk later, the mice were sacrificed and body weight loss was evaluated. Fractions indicate occurrence in the samples.

Animal Experimentation

Female BALB/c nu/nu mice were purchased from Clea Japan (Tokyo, Japan) and maintained under a specific pathogen-free condition. Six- to 8-wk-old mice were used. They were housed in filter-protected cages and reared on sterile water. The ambient light condition was controlled artificially by a 12-h light/dark cycle. All procedures involving animals and their care in this study were approved by the Committee for Ethics in Animal Experimentation of the Yasuda Women's University and the National Cancer Center Institute in accordance with institutional and Japanese Government Guidelines for Animal Experiments.

Isolation of Cachexia-Inducing Cell Lines

Following s.c. inoculation, only 10% to 20% of the MKN-45 and Sui70 tumor-bearing mice showed body weight loss. In a preliminary in vivo study of tumor growth, 1×10^6 MKN-45 cultured cells were inoculated s.c. into BALB/c nu/nu mice. After confirming tumor growth and body weight loss, the mice were sacrificed and tumor tissues were removed under sterile conditions for in vitro cultivation. The obtained specimens were washed 5 times in RPMI-1640 medium containing 500 IU/mL penicillin G sodium and 500 mg/mL streptomycin sulfate. The tumor tissues were trimmed to remove necrotic tissue debris and then minced with a scalpel. Next, 10 to 15 pieces of tissues were transferred into 60-mm culture dishes with 2 mL RPMI-1640 medium containing 20% FBS. The dishes were left undisturbed for 10 h at 37°C in a 5%CO_2/95% air atmosphere. After 10 h,

RPMI-1640 medium with 10% FBS, 100 IU/mL penicillin G sodium, and 100 mg/mL streptomycin sulfate was added to the dishes. After 7 to 14 days, cells were trypsinized (0.05% trypsin and 0.02% EDTA) to selectively remove overgrowing fibroblasts. Half the volume of the culture medium was changed on average every 4th day. After 4 to 6 wk of cultivation, the grown tumor cells (1×10^6) were reimplanted s.c. into mice. Cachexia-inducing tumor cells were removed from these mice, cultured, and then implanted into naïve mice. This process was repeated multiple times to isolate highly potent cachexia-inducing cell lines, and mice subjected to implantation with selected cells showed cachectic weight loss and body wasting. Cells inducing cancer cachexia steadily were isolated after 10 cycles of stepwise selection. The newly established cell line MKN45cl85 was used in the present study.

Analysis of Tumorigenicity and Tumor Growth

The tumorigenicity and cachexia-inducing ability of MKN-45 and MKN45cl85 cell lines were tested by s.c. injection into mice (1×10^6 cells suspended in 100 μL PBS). The tumor was measured in 2 dimensions with calipers, and the volume of each tumor was calculated according to the equation $(L \times W^2)/2$ (L = length, W = width). At intended schedules of survival, or when moribund, the mice were sacrificed and various organs were macroscopically examined for metastasis and then processed for histological examination, as described previously (19).

Establishment of Cachexia-inducing Peritoneal Metastatic Cell Lines

The MKN45cl85 cell line ($1 \times 10^6/50$ μL) was implanted orthotopically under the serosal membrane in the greater curvature of the antrum in BALB/c nu/nu mice, according to a previously described in vivo stepwise selection method (10,22). After 8 wk, the mice were killed and autopsied. The stomach, regional lymph nodes, liver, and other organs were resected to evaluate the metastatic potential of this cell line and processed for routine histopathological examination. Orthotopic implantation of MKN45cl85 cells caused ascites formation in a few animals. We repeated cycles of isolation of ascetic tumor cells and orthotopic reimplantation of these cells into animals to isolate highly metastatic cells with a strong capability of inducing peritoneal dissemination. In the same way, the 85As2 cell line was established in 11 cycles of stepwise selection.

In Vivo Photon Counting Analysis

First, the luciferase gene was inserted into the MSCVIRES-GFP vector. To generate an RD114-pseudotyped retrovirus, the Lipofectamine-Plus reagent (Invitrogen, Carlsbad, CA) was used to transfect 293T cells with the expression vectors for luciferase, pEQ-PAM3(-E), and pRDF (obtained from the St. Jude Vector Development and Production Shared Resource, Memphis, TN). Conditioned medium containing the retroviruses was harvested from transfected 293 cell cultures and stored at $-80°$C until use. 85As2 cells were transformed in virus-conditioned medium with 4 mg/mL polybrene (Sigma-Aldrich, St Louis, MO) in retronectin-precoated wells (Takara, Kyoto, Japan). Transformed cells showing high GFP expression levels were separated using a FACS Aria cell sorter (Becton Dickinson, Franklin Lakes, NJ). The competent 85As2 cells carrying the luciferase gene was named 85As2mLuc.

Second, orthotopic implantation of 1×10^6 85As2mLuc cells was conducted in 8-wk-old female BALB/c-nu/nu mice (day 0) as described previously (10). To assess the tumorigenicity of 85As2mLuc cells, bioluminescence signals from 85As2mLuc cells implanted into mice were monitored after i.p. injection of D-luciferin (150 mg/kg) using the IVIS system Lumina series (Caliper Life Sciences, Hopkinton, MA) as described previously (20,22). During the entire course of monitoring, the animals were kept under isoflurane anesthesia. The tumor volume was identified as the regions of interest (ROI) of bioluminescence and the total photon counts were quantified using the Living Image acquisition and Analysis Software (Caliper Life Sciences). The tumor volume (or ROI) was measured every 7th day and the proliferative growth was determined on the basis of bioluminescence signals by subtracting the value on postimplantation day 1. The tumor volume in each group was expressed as the average values of the total photon counts (22). At the end of the in vivo study, various organs were dissected, examined macroscopically for metastatic foci, and processed for histopathological examination.

Effect of Isoflavones on Tumor Cell Growth In Vitro and In Vivo

Daidzein and genistein were purchased from Sigma-Aldrich and Nagara Science (Gifu, Japan). Isoflavone aglycone Agly-Max (Nichimo Co, Tokyo, Japan) was prepared from soybeans fermented with Koji fungus (*Aspergillus awamori*) and consisted of daidzein, genistein, and glycitein aglycone at a ratio of 7:1:2 (23).

To examine the effects of these isoflavones on in vitro proliferation of cancer cells, each flavonoid compound was applied onto 1-day cultures of MKN45cl85 and 85As2mLuc cells seeded initially in 24-well plates at 1×10^4 cells/mL per well. Isoflavones were first dissolved in DMSO and then used by diluting in culture medium (final concentrations: 100 μM daidzein, 200 μM genistein, and 200 μM AglyMax). On days 2 to 5, cultured cells were trypsinized, collected, and counted to assess the bioactive effects on cell proliferation. The growth rate was also determined by using a crystal violet dye elution (CVE) assay, as described previously (17). An equal volume of DMSO was added to control cultures and no measurable effect was detected on cell growth.

In experiments using either the MKN45cl85 s.c. implantation model or the 85As2mLuc orthotopic implantation model, Agly-Max, daidzein, and genistein (400 μg/0.1 mL per head per day) were injected i.p. every other day starting 2 days before implantation surgery (12 times in total). Control animals were given the same vehicle (DMSO). Tumor growth (s.c.) was measured weekly with calipers (as tumor diameter). The 85As2mLuc tumor growth was monitored by in vivo photon counting analysis 1 day after orthotopic implantation. Food and water were available ad libitum. The mice were observed daily for clinical signs and mortality. Body weight and food consumption were measured weekly. Three or 4 wk later, the mice were sacrificed and tumors grown in the hosts were removed and weighed.

Statistical Analysis

All numerical data are expressed as means ± SE. Data of cytokine levels in culture supernatants or mouse sera, tumor size, and body weight were analyzed using Student's t-test. The survival rate of mice in in vivo experiments was analyzed by Cox-Mantel test. P values less than 0.05 were considered statistically significant.

RESULTS

Isolation of Cachexia-inducing Stomach Cancer Cell Lines

Table 1 shows cancer cachexia-inducing cell lines in terms of body weight loss in mice. Tumor growth was observed in all mice bearing a xenograft, but cachectic weight loss was observed in mice implanted with MKN-45 stomach cancer cells, as well as Sui70 pancreatic cancer cells (19). A highly competent cachexia-inducing tumor cell line was only isolated from the MKN-45 human stomach cancer cell line according to the

protocol described in the **Materials and Methods** section and labeled MKN45cl85.

Subcutaneous implantation of MKN45cl85 cells induced rapid tumor growth in mice as early as 3 wk after surgery (Fig. 1A). The weight loss caused by cancer cachexia set out as the tumor growth plateaued. The mice appeared to get into a cachectic condition, accompanied by decreased activity, xeroderma, and anorexia in 90% to 100% of the mice within 3 to 5 wk postimplantation (Table 2). The initial sign of cachexia depends on the number of inoculated cells. Tumor tissues grown as large as 10 mm in diameter resulted in critical conditions of cancer cachexia in mice, and surgical removal of the tumors resulted in the restoration of healthy conditions (Fig. 1B and 1C). Moreover, the xenograft of MKN45cl85 cells in the mice reduced adipose tissue and musculature volumes (Fig. 1C, lower panel).

Isolation of Cachexia-inducing Peritoneal Metastatic Cell Lines

The MKN45cl85 cancer cell line described above had no metastatic competence to peritoneal dissemination. In xenograft experiments of MKN45cl85 cells, ascitic tumors developed in 20% to 30% of host mice. Accordingly, another cancer cell line was newly isolated from these ascitic tumors of mice by repeated isolation of competent metastatic cells in vitro and subsequent xenografting in mouse. The new metastatic cell line named 85As2, which is derived from MKN45cl85 cancer cells, possessed a high capability for inducing peritoneal dissemination (Table 2). For further study, the luciferase gene was introduced into 85As2 tumor cells and the resultant cells were named 85As2mLuc. 85As2mLuc cells were able to cause cancer cachexia in 100% of mice after 3 to 5 wk, by either orthotopic or subcutaneous implantation (Fig. 1D). The musculature and adipose tissue weights in cachectic mice at 4 wk after subcutaneous implantation were remarkably and significantly reduced compared with those of the nontumor-bearing group [gastrocnemius muscle (g): nontumor-bearing, 0.1252 ± 0.0074, $n = 5$, and tumor-bearing, 0.0757 ± 0.0049, $n = 5$, $P < 0.001$; epididymal fat (g): nontumor-bearing, 0.1056 ± 0.0181, $n = 5$ and tumor-bearing, 0.0000 ± 0.0000, $n = 5$).

Characterization of 2 Cachexia-inducing Cancer Cell Lines

The MKN45cl85 cell line, as well as the parental MKN-45 cell line, had round or spindle-shaped-like cell morphology, tended to aggregate loosely, and showed a characteristic pattern of attaching to the bottom of the flask. On the other hand, 85As2mLuc cells were round and nonadherent (Fig. 2, upper column). A clear difference was observed with regard to adhesion to the bottom of the dishes.

The supernatants collected from MKN45cl85, 85As2mLuc, and MKN-45 cell line cultures were processed for examining cachectic cytokines produced by the cells (Table 2). IL-6, IL-10, TGF-α, TGF-β, and TNF-α were not detected in all cell lines. In addition, these cytokines were not detected in the sera of cachectic mice that received s.c. implantation of MKN45cl85 and 85As2mLuc cells.

The number of postimplantation survival days of mice was relatively smaller in 85As2mLuc cells than in MKN45cl85 and MKN-45 cells (Table 2). When the 3 cancer cell lines were implanted s.c., mice developed tumors in situ but exhibited no metastasis to other organs. On the other hand, orthotopic implantation of the 3 cell lines caused metastases to various organs. Of the 3 cell lines, only 85As2mLuc cancer cells caused peritoneal dissemination of the cells to the mesentery and omentum in mice. Metastases of 85As2mLuc cancer cells to neighboring lymph nodes and liver were also frequently observed (Table 2). Mice implanted with 85As2mLuc cells appeared to be more severely affected than those receiving MKN45cl85 and MKN-45 cells.

Effects of Isoflavones on Proliferation of Cachexia-inducing Cancer Cells In Vitro

Effects of the 3 types of isoflavones on cancer cell proliferation were examined using MKN45cl85 and 85As2mLuc cell lines in vitro (Fig. 2, lower column). After application of the flavonoid compounds, cell proliferation was monitored on a daily basis, using the CVE assay. The inhibitory effects of genistein and AglyMax on proliferation of both cancer cell lines were observed at 1 μM at 72 h after application of the compounds. The inhibitory effects increased as the concentrations of the compounds increased (up to 200 μM). Daidzein was relatively less effective because it could inhibit proliferation of both cancer cell lines at a concentration as high as 100 μM (Fig. 2, lower column). This inhibitory effect of daidzein appeared from 24 h through 96 h after application of the compound, with a gradual increase in the inhibition as time proceeded. Thus, the 3 isoflavones exerted inhibitory effects on proliferation of the 2 cachexia-inducing cancer cell lines.

Suppressive Effects of Isoflavones on Tumor Growth and Cachexia In Vivo

The antineoplastic and anticachectic activities of the isoflavones were investigated using 2 xenograft implantation models leading to cancer cachexia (Table 3 and Fig. 3). First, effects of 3 types of isoflavones on tumor growth and cachexia were examined in mice that underwent s.c. implantation of MKN45cl85 cells (Fig. 3A and 3B). Of the 3 flavonoid compounds, AglyMax significantly inhibited proliferative growth of the xenografted cells (Fig. 3A). Daidzein and genistein suppressed the proliferation of cancer cells to a lesser extent in mice. The extent of the inhibitory effect of isoflavones against tumor growth was graded as AglyMax > daidzein > genistein (Fig. 3A). We also examined changes in body weight in these isoflavone-treated mice. The anticachectic activities of the 3 isoflavones in terms of the body weight loss in these s.c. implantation mouse models are shown in Fig. 3B. AglyMax- and daidzein-treated mice did not show cachexia-associated body
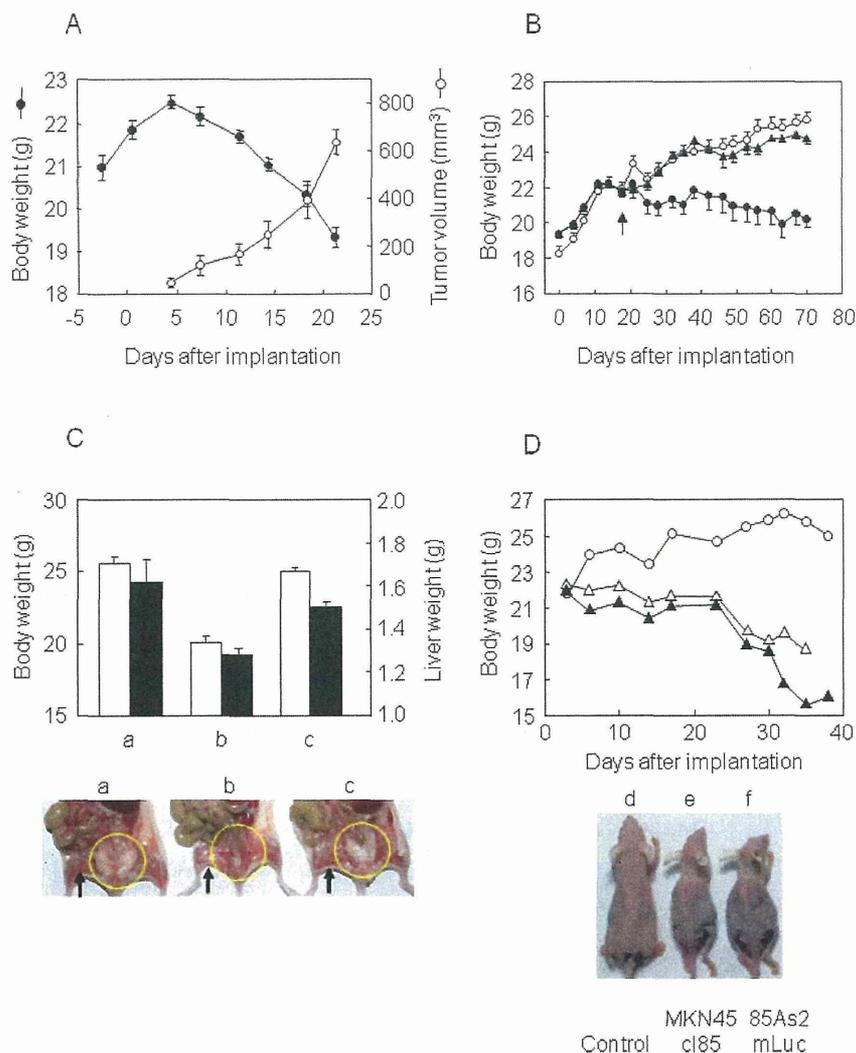
FIG. 1. Body weight and tumor growth of mice bearing MKN45cl85 and 85As2mLuc cancer cell lines. **A:** Growth curves of body weight of mice and tumor volume. MKN45cl85 cells were s.c. implanted into left and right flanks (1×10^6 cells/each site) on Day 0. Body weight (•) and tumor volume (○) were measured periodically. $n = 5$. **B:** Growth curves of body weight of mice. MKN45cl85 cells were implanted s.c. into the right flank (1×10^6 cells/site) on Day 0. One group of mice carried the tumor during the experiment (•). In another group (▲), tumors that grew as large as 10 mm in diameter were removed on Day 18 (arrow). The control group consisted of age- and sex-matched mice (○). $n = 5$. **C:** Body weight (open bar) and liver weight (solid bar) in histograms and macroscopic views of autopsies of the lower halves of mouse bodies at 3 wk after s.c. implantation of MKN45cl85 cells. In both upper and lower panels, (a) age- and sex-matched control, (b) tumor bearing, and (c) tumor-removed mice. Apparent changes in the volume of the parametrical fat mass (yellow circle) and hind limb musculature (arrow) were recognized. $n = 5$. **D:** Body weight curves and dorsal views of mice that underwent orthotopic implantation of MKN45cl85 (△, e) and 85As2mLuc (▲, f) cancer cells (1×10^6 cells) into subserous regions of the stomach on day 0. Control mice were age- and sex-matched (○, d) (Color figure available online).

weight loss, but cachectic weight loss was observed in genistein-treated mice.

Next, we examined tumor growth and cachexia-suppressive activities of isoflavones in mice, in which 85As2mLuc cells were implanted orthotopically. This mouse model supported the results obtained in the experiment of s.c. implantation of MKN45cl85 cells (Table 3 and Fig. 3). The extent of the antitumor effect of the isoflavones was graded as AglyMax >

daidzein > genistein (Fig. 3C and 3E). Furthermore, mitosis of these isoflavone-treated 85As2mLuc tumors was observed histopathologically. The mitotic index was dependent on the antitumor potential of each isoflavone (Table 3).

With regard to the characteristics of the mouse model in which 85As2mLuc cells were implanted orthotopically followed by treatment with AglyMax and daidzein, cancer cachexia was not observed and neither was body weight loss, decreased

TABLE 2
Biological properties of newly isolated cachexia-inducing sublines and parent MKN-45 cell line

| | Production of cytokine[†] | | | | | Xenotransplantation in nude mice | | | | | |
| | | | | | | | | | Metastasis[§] | | |
Cell line	IL-6 (ng)	IL-10 (ng)	TNF-α (ng)	TGF-α (pg)	TGF-β1 (ng)	Cachexia[‡] induction	Tumor[‡] formation	Survival[‡] time (days)	Peritoneal dissemination	Ascites formation	Liver/ lymph node
MKN-45	ud	ud	ud	ud	ud	3/10	10/10	38.8 (22–55)	2/10	0/10	0/10
MKN45cl85	ud	ud	ud	ud	ud	9/9	9/9	40.5 (23–53)	6/10	0/10	0/10
85As2mLuc	ud	ud	ud	ud	ud	10/10	10/10	23.3 (15–37)	10/10	7/10	8/10

ud = undetectable, below the minimum detection limit of the assay kit.

[†]Supernatant was collected from 48 h incubation cultures. Data of interleukin (IL)-6, IL-10, tumor necrosis factor (TNF)-α, and TGF-β1 are expressed as ng/10^6 cells; data of TGF-α are expressed as pg/10^6 cells.

[‡]Mice were implanted s.c. into left and right flank (1×10^6 cells/site).

[§]Mice were implanted orthotopically into subserous regions of the stomach (1×10^6 cells). Data of the occurrence are shown by fractions; numerators of each fraction indicate positive numbers in the samples (denominators).

activity, skin dryness, and anorexia. The mean body weights in the AglyMax-treated, daidzein-treated, and control group were 20.74 ± 0.47, 19.50 ± 0.75, and 17.24 ± 0.19 g, respectively, on Day 26 (Table 3 and Fig. 3D, $P = 0.05$). Histological examinations of coelomic viscera (liver, lung, heart, kidney, adrenal gland, and ovary) of AglyMax- and daidzein-treated mice showed that they were normal. In contrast, body weight loss was seen in both vehicle- and genistein-treated mice.
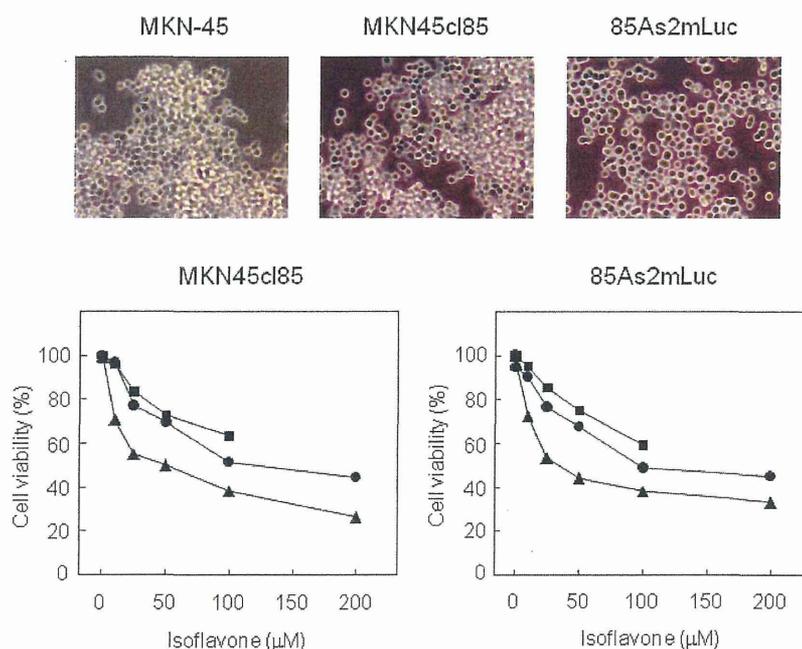

FIG. 2. Phase-contrast photomicrographs and dose-dependent viability curves of cachexia-inducing cancer cell lines under inhibitory influence of 3 types of isoflavones. The inhibitory effects of isoflavones on the viability of cancer cells were dose-dependent. Original magnification, ×200. MKN45cl85 and 85As2mLuc cells were initially seeded at 1×10^4 cells/mL per well, incubated overnight, and then exposed to different types of isoflavones, genistein (▲), daidzein (■) and AglyMax (●). After 74 h, cell viability was determined by using a crystal violet dye elution assay. A higher concentration (200 μM) of daidzein was not available because of its poor solubility. (Color figure available online).

TABLE 3

Effects of various isoflavones on tumor growth and body weight in orthotopic implantation: 85As2mLuc model

	Tumor growth[†]		
	Volume[‡]		
Isoflavones	photon counts ($\times 10^8$)	Mitotic[§] index (%)	Body weight (g)
Control	34	4.61	17.24 ± 0.19
Genistein	17	3.56	18.00 ± 0.31
Daidzein	8	2.59	19.50 ± 0.75
AglyMax	5.9	0.96	20.74 ± 0.47

[†]Mice were sacrificed on Day 26 after orthotopic implantation into subserous regions of the stomach (2×10^6 cells).

[‡]Tumor volume was measured by in vivo photon counting analysis.

[§]Mitotic index of the stomach tumor was calculated using histological section (No. of mitotic cells/2000 tumor cells).

Student's t-test: daidzein group vs. control group, $P < 0.05$; AglyMax group vs. control group, $P < 0.01$. $n = 5$.

Effects of Isoflavones on Survival and Metastasis in the Model of Orthotopic Implantation of 85As2mLuc Cells

Effects of isoflavones on survival and metastasis were examined in the 85As2mLuc model with metastatic stomach cancer, in which the tumor take rate was 100%, followed by vigorous tumor growth and subsequent death until 60 days after tumor implantation without treatment of isoflavones. The highly aggressive nature of the tumor is summarized in Table 2. Administration of isoflavones to 85As2mLuc tumor-bearing mice resulted in prolonged survival (Table 4). Metastasis of 85As2mLuc tumors to remote organs/tissues was not inhibited in mice. The volume of ascites from mice on sacrifice was similar between isoflavone- and DMSO-treated control groups. However, treatments with different isoflavones improved the median survival rate of mice in comparison with those treated with vehicle (Table 4). The effects on the survival rate of mice with regard to efficacy of isoflavones were graded as AglyMax > daidzein > genistein (Fig. 3F).

DISCUSSION

Stomach cancer ranks second in incidence and mortality worldwide, despite its overall decline (24). Asian countries with a particularly high incidence of this cancer include Japan, Korea, and China. Stomach cancer patients have a high incidence of cachexia (incidence of weight loss, about 83%) (25). Obtaining greater knowledge about the pathophysiology of cachexia for stomach cancer is urgently needed to establish methods for early diagnosis and effective treatment, including effective anticachectic therapy, of this debilitating disease. Toward this end, extensive in vivo or in vitro studies using suitable experimental models are indispensable. Animal models would be useful for analyzing cancer-associated events inside the body

and for evaluating the pharmacodynamic effects of candidate anticachectic agents, if they mimicked human cases of cachexia. The orthotopic implantation mouse models of stomach cancer-derived tumors established in the present study demonstrated the development of cancer cachexia and the metastasis of these tumors to various sites at high frequency and the development of ascites within a relatively short period. These mouse models also showed a favorable response to anticancer agents, isoflavones, which may pave the way for designing manipulations to clarify the pathogenesis of cancer cachexia.

In vivo studies of cachexia of stomach cancer may be expected to play a pivotal role in understanding the nature and behavior of the tumor cells inside the body, in particular with regard to interaction with the host. We isolated a cachexia-inducing (as body weight loss) subline with nonmetastatic potential, MKN45cl85, from the stomach cancer cell line MKN-45. Moreover, we were able to isolate another cell line, 85As2mLuc, which exhibited very aggressive growth in mice, accompanied by the induction of cancer cachexia. 85As2mLuc tumors are usually more invasive and highly metastatic and associated with poor prognosis. Xenograft mouse models have attracted attention as useful cachexia models because they reflect the malignant stages of stomach cancer in the clinical setting.

Stomach cancer patients have high incidence of cachexia; however, there are few experimental cachexia models using human stomach cancer. In the present study, we screened 15 different human stomach cancer cell lines and then established 2 cachexia-inducing cancer cell lines (MKN45cl85 and 85As2mLuc) from MKN-45. It is speculated that the differences in the potency to cause cancer cachexia between these 2 cell lines and other stomach cancer cell lines may be associated with the production of the cachectic factors such as cytokines by cancer cells or host cells. In humans and rodent models, there is increasing evidence that cytokines, including TNF-α, IL-1, IL-6, IL8, IL-10, TGF-α, TGF-β, and vascular endothelial growth factor (VEGF) may be involved in the cause or development of cancer cachexia (26–32). Some investigators have found that higher IL-6 levels in patients with nonsmall cell lung, pancreatic, and prostatic cancers were associated with weight loss (33–35). In Phase I and II trials, treatment with a humanized anti-IL-6 antibody ameliorated nonsmall cell lung cancer-related cachexia (36). In addition, a human–mouse chimeric monoclonal antibody, which blocks human IL-6 but not mouse IL-6, ameliorated body weight loss in cancer cachexia mouse models inoculated with human melanoma cells or human prostate tumor cells (37). Thus, these studies have shown that IL-6 may be the cause or the potential therapeutic targeting of cancer cachexia. In the present study, secretion of IL-6 was not detected in the culture supernatants and sera of MKN45cl85 and 85As2mLuc tumor-bearing cachectic mice. On the other hand, other data have raised doubts as to whether IL-6 was an independent cachectic factor (38). Therefore, these results suggest that other factors but not IL-6 may be involved in cachexia development of the present model (39,40). Further study is necessary to investigate which
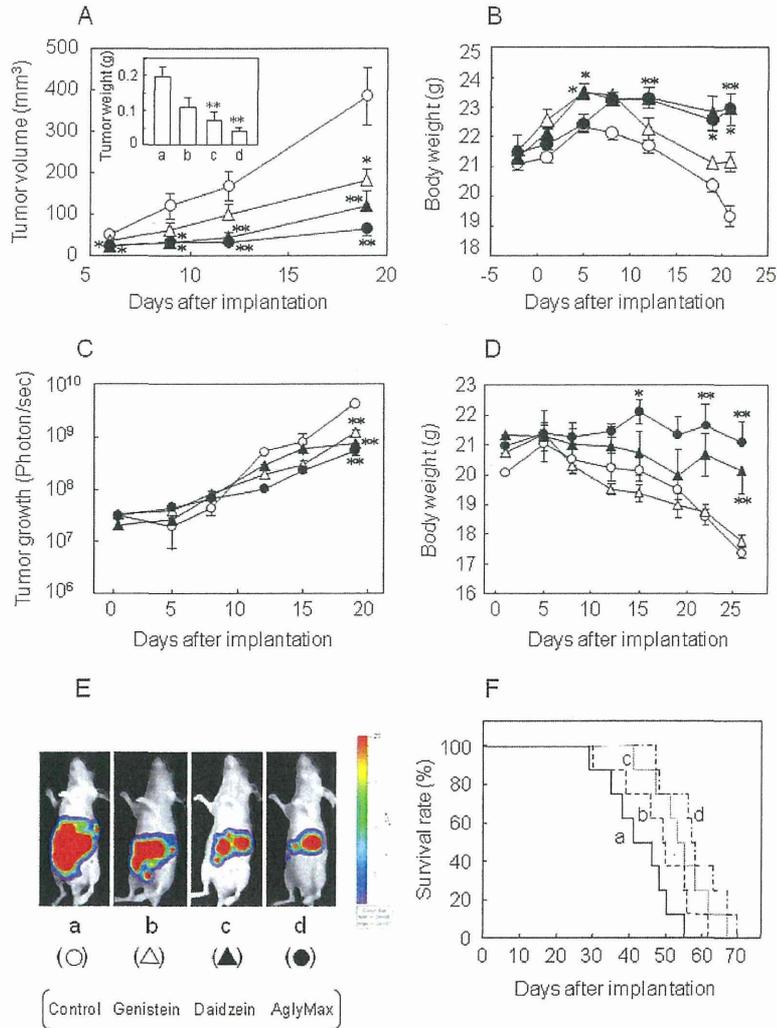
FIG. 3. Inhibition of tumor growth and body weight loss by isoflavones in mice bearing cachexia-inducing MKN45cl85 and 85As2mLuc cells. Growth curves of tumors (A, C, and E), body weight (B and D), and days of survival (F) in mice in which MKN45cl85 cells were implanted (s.c.) into right and left flanks (1×10^6 cells/each site) and in which 85As2mLuc cells were implanted orthotopically. $n = 6$. Cancer cells were implanted on Day 0. A: Growth of tumor volume (tumor weight, inset) of MKN45cl85 cells in mice was inhibited and (B) their body weight increased by administering isoflavones (400 μg/mouse per day) i.p. every other day, starting from 2 days before implantation. Twelve shots during the experiment (4.8 mg/head). Genistein ($\triangle$, b), daidzein ($\blacktriangle$, c), and AglyMax ($\bullet$, d). Control mice received equal amounts of vehicle ($\circ$, a). C: Growth curves of tumor size and (D) body weight in mice that received orthotopic implantation of 85As2mLuc cells (2×10^6 cells) into subserous regions of the stomach on Day 0. Growth of 85As2mLuc cell tumors was measured by using the IVIS system. Mice: control ($\circ$, a), genistein ($\triangle$, b), daidzein ($\blacktriangle$, c), and AglyMax ($\bullet$, d). *$P < 0.05$, **$P < 0.01$ compared with the values for the control on the corresponding days. E: Photographs showing in vivo quantitative photon counting analysis utilizing bioluminescence signals on day 26 after orthotopic implantation of 85As2mLuc cells. Isoflavones were administered i.p. every other day, starting from 2 days before implantation. The size of tumors in mice was indicated by color (red is intense and blue is the opposite). Mice: control ($\circ$, a) genistein ($\triangle$, b), daidzein ($\blacktriangle$, c), and AglyMax ($\bullet$, d). F: A chart showing days of survival in mice after orthotopic implantation of 85As2mLuc cancer cells (1×10^6 cells) in subserous regions of the stomach. Surgery was carried out on Day 0. Isoflavones were administered i.p. every other day, starting from 2 days before implantation. The efficacy of different types of isoflavones on survival in mice was graded in intensity. (a) vehicle, (b) genistein, (c) daidzein, and (d) AglyMax. The groups consisted of 8 mice each. Cox-Mantel test: daidzein group vs. control group, $P = 0.06$; AglyMax group vs. control group, $P = 0.01$. (Color figure available online).

cachectic factors contributed to the different potency to cause cachexia.

Epidemiologic, in vitro, and in vivo studies have provided evidence for the hypothesis that certain soy phytochem-icals, especially soy isoflavones, have antitumorigenic properties (12–15,17,41,42). In the present study, we have assessed the anticachexia effects of isoflavones using 2 stomach cancer models. We demonstrated that administration of isoflavones

TABLE 4

Effect of various isoflavones on survival and metastasis in an orthotopic implantation: 85As2mLuc model

		Metastasis[‡]			
Isoflavones	Survival[†] time (days)	Ascites[§] formation	Peritoneal dissemination	Lymph node (regional)	Liver surface
Control	42.8 (29–55)	6/8	8/8	6/8	6/8
Genistein	48.4 (30–62)	5/8	8/8	5/8	5/8
Daidzein	54.3 (41–67)	6/8	8/8	5/8	5/8
AglyMax	58.3 (47–70)	5/8	8/8	5/8	5/8

[†]Mice were implanted orthotopically into the subserous regions of stomach cancer cells (1×10^6 cells). Mice were sacrificed on day 70 after implantation or when moribund.

[‡]Data of the metastasis are shown by fraction; numerators of each fraction indicate positive numbers in the samples (denominators).

[§]Ascites formation and body weight were assessed at the time of death (body weight includes ascites).

mitigated cachexia and prolonged the survival of the host by mechanisms mainly dependent of their antiproliferative action. However, the mechanism causing the shorter survival associated with cachexia has not been clarified yet. Suppression of cancer cachexia may be due to inhibition of tumor proliferation by isoflavones. We have previously found that 11 cultured human stomach cancer cell lines undergo morphological changes and internucleosomal DNA fragmentation characteristic of apoptosis after exposure to isoflavone derivatives (biochanin A, daidzein, and genistein) in vitro and in vivo (17). We and others have also shown that these isoflavones induce apoptosis in a specific cell cycle phase (43,44). Biochanin A and daidzein induce G_1 arrest, whereas genistein blocks at G_2-M in cancer cell lines (43). Accordingly, our observations indicate that 3 isoflavones (AglyMax, daidzein, and genistein) mitigate cachexia and inhibit tumor proliferation of stomach cancer cell lines in vivo through activation of a signal transduction pathway for apoptosis. Moreover, quercetin, a flavonoid compound abundantly present in fruits, vegetables, wine, and tea has several activities such as antiproliferative and anticancer activities. Camargo et al. (45), showed inhibition of tumor growth, prolonged survival, decrease in matrix metalloproteinase-2 and VEGF levels, and reduction of cachexia in walker 256 tumor-bearing rats treated with quercetin. Their results strongly support the anticancer function, including cachexia, of this flavonoid compound. We hypothesize that increased intake of soy bioactive components may provide an effective nutritional regimen for the prevention of stomach cancer progression because soy bioactive components can exert their effects via both blood circulation and, in particular, direct contact with the mucosa of the stomach.

On the other hand, during the past decade, increasing evidence has shown that dysregulation of inflammatory pathways contributes to the development of cachexia (46). The nuclear factor (NF)-κB is a major mediator of inflammatory pathways. Therefore, antiinflammatory agents that can modulate NF-κB activation and inflammatory pathways may have potential in improving cancer-related symptoms such as cachexia (47, 48).

More recently, studies using in vitro and in vivo models have demonstrated that isoflavones inhibit NF-κB activation and modulate inflammatory pathways (49). Further investigations are needed to elucidate the mechanisms responsible for cancer cachexia.

In conclusion, we isolated 2 cachexia-inducing sublines (MKN45cl85 and highly metastatic 85As2mLuc) from the human stomach cancer cell line MKN-45. These cell lines may provide a good tool to study the development of cancer cachexia and malignant progression of human stomach cancer. To our knowledge, the MKN45cl85 and metastatic 85As2mLuc cell lines are the first stomach cancer cell lines reported to induce cachexia at high frequency in mice. These cachectic animal models are worthy of further study to explore the treatment of stomach cancer-induced cachexia. Our results demonstrated that isoflavones could exert therapeutic efficacy on amelioration of cancer cachexia in the host. Nevertheless, the results of this study also indicate that a longer period of treatment is required to maintain these effects.

ACKNOWLEDGMENTS

no conflicts of interest that would prejudice the impartiality of this scientific work.

REFERENCES

1. Loberg RD, Bradley DA, Tomlins SA, Chinnaiyan AM, and Pient KJ: The lethal phenotype of cancer: the molecular basis of death due to malignancy. *CA Cancer J Clin* **57**, 225–241, 2007.

2. Fearon K, Strasser F, Anker SD, Bosaeus I, Bruera E, et al.: Definition and classification of cancer cachexia: an international consensus. *Lancet Oncol* **12**, 489–495, 2011.

3. Evans WJ, Morley JE, Argiles J, Bales C, Baracos V, et al.: Cachexia: A new definition. *Clin Nutr* **27**, 793–799, 2008.

4. Muscaritoli M, Bossola M, Aversa Z, Bellantone R, and Fanelli FR: Prevention and treatment of cancer cachexia: new insights into an old problem. *Eur J Cancer* **42**, 31–41, 2006.

5. Dewys WD: Weight loss and nutritional abnormalities in cancer patients: incidence, severity and significance. In: *Clinics in Oncology*, Calman KC, Fearon KCH, eds. London: Saunders, 1986, 251–261.

6. Laviano A, Meguid MM, Inui A, Muscaritoli M, and Rossi-Fanelli F: Therapy insight: cancer anorexia-cachexia syndrome-when all you can eat is yourself. *Nat Clin Prac Oncol* **2**, 158–165, 2005.

7. Mori T, Fujiwara Y, Yano M, Tamura S, Yasuda T, et al.: Prevention of peritoneal metastasis of human gastric cancer cells in nude mice by S-1, a novel oral derivative of 5-fluorouracil. *Oncology* **64**, 176–182, 2003.

8. Tanaka F, Tominaga K, Shiota M, Ochi M, Kuwamura H, et al.: Interleukin-10 gene transfer to peritoneal mesothelial cells suppresses peritoneal dissemination of gastric cancer cells due to a persistently high concentration in the peritoneal cavity. *Cancer Gene Ther* **15**, 51–59, 2008.

9. Fidler IJ, Naito S, and Pathak S: Orthotopic implantation is essential for the selection, growth and metastasis of human renal cell cancer in nude mice. *Cancer Metastasis Rev* **9**, 149–165, 1990.

10. Yanagihara K, Takigahira M, Tanaka H, Komatsu T, Fukumoto H, et al.: Development and biological analysis of peritoneal metastasis mouse models for human scirrhous stomach cancer. *Cancer Sci* **96**, 323–332, 2005.

11. Wei H, Cai Q, and Rahn RO: Inhibition of UV light- and Fenton reaction-induced oxidative DNA damage by the soybean isoflavone genistein. *Carcinogenesis* **17**, 73–77, 1996.

12. Booth C, Hargreaves DF, Hadfield JA, McGown AT, and Potten CS: Isoflavones inhibit intestinal epithelial cell proliferation and induce apoptosis in vitro. *Br J Cancer* **80**, 1550–1557, 1999.

13. Fotsis T, Pepper M, Adlercreutz H, Fleischmann G, Hase T, et al.: Genistein, a dietary-derived inhibitor of in vitro angiogenesis. *Proc Natl Acad Sci* **9**, 2690–2964, 1993.

14. Okura A, Arakawa H, Oka H, Yoshinari T, and Monden Y: Effect of genistein on topoisomerase activity and on the growth of [Val 12]Ha-ras-transformed NIH 3T3 cells. *Biochem Biophys Res Commun* **30**, 183–189, 1988.

15. Akiyama T, Ishida J, Nakagawas S, Ogawara H, Watanbe S: Genistein, a specific inhibitor of tyrosine-specific protein kinase. *J Biol Chem* **25**, 5592–5595, 1987.

16. Motoyama T, Hojyo H, and Watanabe E: Comparison of seven cell lines derived from human gastric carcinomas. *Acta Path Jap* **36**, 65–83, 1986.

17. Yanagihara K., Ito A, Toge T, and Numoto M: Antiproliferative effects of isoflavones on human cancer cell lines established from the gastrointestinal tract. *Cancer Res* **53**, 5815–5821, 1993.

18. Yanagihara K, Tanaka H, Takigahira M, Ino Y, Yamaguchi Y, et al.: Establishment of two cell lines from human gastric scirrhous carcinoma that possess the potential to metastasize spontaneously in nude mice. *Cancer Sci* **95**, 575–582, 2004.

19. Yanagihara K, Takigahira M, Tanaka H, Arao T, Aoyagi Y, et al.: Establishment and molecular profiling of a novel human pancreatic cancer panel for 5-FU. *Cancer Sci* **99**, 1859–1864, 2008.

20. Yanagihara K, Tsumuraya M, Takigahira M, Mihara K, Kubo T, et al.: An orthotopic implantation mouse model of human malignant pleural mesothelioma for in vivo photon counting analysis and evaluation of the effect of S-1 therapy. *Int J Cancer* **126**, 2835–2846, 2010.

21. Yanagihara K and Tsumuraya M: Transforming growth factor β_1 induces apoptotic cell death in cultured human gastric carcinoma cells. *Cancer Res* **52**, 4042–4045, 1992.

22. Yanagihara K, Takigahira M, Takeshita F, Komatsu T, Nishio K, et al.: A photon counting technique for quantitatively evaluating progression of peritoneal tumor dissemination. *Cancer Res* **66**, 7532–7539, 2006.

23. Xu JW, Yasui N, Ikeda K, Pan WJ, Watanabe J, et al.: Isoflavones regulate secretion of leukemia inhibitory factor and transforming growth factor-β and expression of glycodelin in human endometrial epithelial cells. *J Endocrinology* **196**, 425–433, 2008.

24. Parkin DM, Bray F, Ferlay J, and Pisani P: Estimating the world cancer burden: Globocan 2000. *Int J Cancer* **94**, 153–156, 2001.

25. Bruera E: ABC of palliative care. Anorexia, cachexia and nutrition. *Br Med J* **315**, 1219–1222, 1997.

26. Tisdale MJ: Mechanisms of cancer cachexia. *Physio Rev* **89**, 381–410, 2009.

27. Krzystek-Korpacka M, Matusiewicz M, Diakowska D, Grabowski K, Blachut K, et al.: Impact of weight loss on circulating IL-1, IL-6, IL-8, TNF-α, VEGF-A, VEGF-C and midkine in gastroesophageal cancer patients. *Clin Biochem* **40**, 1353–1360, 2007.

28. Chang JW, Yeh KY, Shen YC, Hsieh JJ, Chuang CK, et al.: Production of multiple cytokines and induction of cachexia in athymic nude mice by a new anaplastic thyroid carcinoma cell line. *J Endocrinology* **179**, 387–394, 2003.

29. Kumar S, Kishimoto H, Chua HL, Badve S, Miller KD, et al.: Interleukin-1α promotes tumor growth and cachexia in MCF-7 xenograft model of breast cancer. *Am J Pathol* **163**, 2531–2541, 2003.

30. Kamoshida S, Watanabe K, Suzuki M, Mizutani Y, Sakamoto K, et al.: Expression of cancer cachexia-related factors in human cancer xenografts: an immunohistochemical analysis. *Biomed Res* **27**, 275–281, 2006.

31. Fujimoto-Ouchi K, Tamura S, Mori K, Tanaka Y, and Ishitsuka H: Establishment and characterization of cachexia-inducing and non-inducing clones of murine colon 26 carcinoma. *Int J Cancer* **61**, 522–528, 1995.

32. Kemik O, Kemik AS, Begenik H, Erdur FM, Emre H, et al.: The relationship among acute-phase response proteins, cytokines, and hormones in various gastrointestinal cancer types patients with cachectic. *Hum Exp Toxicol* **31**, 117–125, 2012.

33. Scott HR, McMillan DC, Crilly A, MaArdle CS, and Milroy R: The relationship between weight loss and interleukin 6 in non-small cell lung cancer. *Br J Cancer* **73**, 1560–1562, 1996.

34. Okada S, Okusaka T, Ishii H Kyogoku A, Yoshimori M, et al. : Elevated serum interleukin-6 levels in patients with pancreatic cancer. *Jpn J Clin Oncol* **28**, 12–15, 1998.

35. Kuroda K, Nakashima J, Kanao K, Kikuchi E, Miyajima A, et al.: Interleukin 6 is associated with cachexia in patients with prostate cancer. *Urology* **69**, 113–117, 2007.

36. Bayliss TJ, Smith JT, Schuster M, Dragnev KH, and Rigas JR: A humanized anti-IL-6 antibody (ALD518) in non-small cell lung cancer. *Expert Opin Biol Ther* **11**, 1663–1668, 2011.

37. Zaki MH, Nemeth JA, and Trikha M: CNTO 328, a monoclonal antibody to IL-6, inhibits human tumor-induced cachexia in nude mice. *Int J Cancer* **111**, 592–595, 2004.

38. Soda K, Kawakami M, Kashii K, and Miyata M: Manifestations of cancer cachexia induced by colon 26 adenocarcinoma are not fully ascribable to interleukin-6. *Int J Cancer* **62**, 332–336, 1995.

39. Inui A, Asakawa A, Bowers CY, Mantovani G, Laviano A, et al.: Ghrelin, appetite, and gastric motility: the emerging role of the stomach as an endocrine organ. *FASEB J* **18**, 439–456, 2004.

40. Hashimoto H, Azuma Y, Kawasaki M, Fujihara H, Onuma E, et al.: Parathyroid hormone-related protein induces cachectic syndromes without directly modulating the expression of hypothalamic feeding-regulating peptides. *Clin Cancer Res* **13**, 292–298, 2007.

41. Hilakivi-Clarke L, Andrade JE., and Helferich W: Is soy consumption good or bad for the breast? *J Nutr* **140**, 2326S–2334S, 2010.

42. Banerjee S, Li Y, Wang Z, and Sarkar FH: Multi-targeted therapy of cancer by genistein. *Cancer Lett* **269**, 226–242, 2008.

43. Yanagihara K, Numoto M, Tauchi H, Akama Y, Yokozaki H, et al.: Genetic status of p53 and induction of apoptosis by radiation or isoflavones in human gastric carcinoma cell lines. *Int J Oncol* **9**, 95–102, 1996.

44. Matsukawa Y, Marui N, Sakai T, Satomi Y, Yoshida M, et al.: Genistein arrests cell cycle progression at G2-M. *Cancer Res* **53**, 1328–1331, 1993.

45. Camargo CA, da Silva ME, da Silva RA, Justo GZ, Gomes-Marcondes MC, and Aoyama H: Inhibition of tumor growth by quercetin with increase of survival and prevention of cachexia in Walker 256 tumor-bearing rats. *Biochem Biophys Res Commun* **406**, 638–642, 2011.

46. Gadgeel SM, Ali S, Philip PA, Wozniak A, and Sarkar FH: Genistein enhances the effect of epidermal growth factor receptor tyrosine kinase inhibitors and inhibits nuclear factor kappa B in nonsmall cell lung cancer cell lines. *Cancer* **115**, 2165–2176, 2009.

47. Raffoul JJ, Wang Y, Kucuk O, Forman JD, Sarker FH, and Hillman GG: Genistein inhibits radiation-induced activation of NF-κB in prostate cancer cells promoting apoptosis and G2/M cell cycle arrest. *BMC Cancer* **6**, 107, 2006.

48. Singh AV, Franke AA, Blackburn GL, and Zhou J-R: Soy phytochemicals prevent orthotopic growth and metastasis of bladder cancer in mice by alterations of cancer cell proliferation and apoptosis and tumor angiogenesis. *Cancer Res* **66**, 1851–1858, 2006.

49. Valsecchi AE, Franchi S, Panerai AE, Rossi A, Sacerdote P, and Colleoni M: The soy isoflavone genistein reverses oxidative and inflammatory state, neuropathic pain, neurotrophic and vasculature deficits in diabetes mouse model. *Eur J Pharmacol* **650**, 694–702, 2011.

Possible involvement of prolonging spinal μ-opioid receptor desensitization in the development of antihyperalgesic tolerance to μ-opioids under a neuropathic pain-like state

Minoru Narita[1], Satoshi Imai[1], Atsushi Nakamura[1], Ayumi Ozeki[1], Megumi Asato[1], Mahardian Rahmadi[1], Yuka Sudo[2], Minoru Hojo[3], Yasuhito Uezono[2,4], Lakshmi A. Devi[5], Naoko Kuzumaki[1] & Tsutomu Suzuki[1]

Department of Toxicology, Hoshi University School of Pharmacy and Pharmaceutical Sciences, Japan[1], Department of Cellular and Molecular Biology, Nagasaki University Graduate School of Biomedical Sciences, Japan[2], Department of Anesthesiology, Nagasaki University Graduate School of Biomedical Sciences, Japan[3], Cancer Pathophysiology Division, National Cancer Center Research Institute, Japan[4] and Department of Pharmacology and Systems Therapeutics, Mount Sinai School of Medicine, New York, NY, USA[5]

ABSTRACT

In the present study, we investigated the possible development of tolerance to the antihyperalgesic effect of μ-opioid receptor (MOR) agonists under a neuropathic pain-like state. Repeated treatment with fentanyl, but not morphine or oxycodone, produced a rapid development of tolerance to its antihyperalgesic effect in mice with sciatic nerve ligation. Like the behavioral study, G-protein activation induced by fentanyl was significantly reduced in membranes obtained from the spinal cord of nerve-ligated mice with in vivo repeated injection of fentanyl. In β-endorphin-knockout mice with nerve ligation, developed tolerance to the antihyperalgesic effect of fentanyl was abolished, and reduced G-protein activation by fentanyl after nerve ligation with fentanyl was reversed to the normal level. The present findings indicate that released β-endorphin within the spinal cord may be implicated in the rapid development of tolerance to fentanyl under a neuropathic pain-like state.

Keywords Fentanyl, mouse, neuropathic pain, opioid tolerance, μ-opioid receptor, spinal cord.

Correspondence to: Minoru Narita and Tsutomu Suzuki, Department of Toxicology, Hoshi University School of Pharmacy and Pharmaceutical Sciences, 2-4-41 Ebara, Shinagawa-ku, Tokyo 142-8501, Japan. E-mail: narita@hoshi.ac.jp and suzuki@hoshi.ac.jp

INTRODUCTION

Although drugs that act on μ-opioid receptor (MOR), such as morphine, fentanyl and oxycodone, have been used clinically as analgesics, these MOR agonists also have undesirable effects, such as tolerance, and physical and psychological dependence (Ventafridda and De Conno, 1981; Raynor *et al.* 1994). It has been considered that opioid tolerance is, in part, the end result of a coordinated balance between processes that govern the desensitization, internalization and resensitization of MORs (Claing *et al.* 2002; Gainetdinov *et al.* 2004). The initial process in these events is the phosphorylation of intracellular domains of MORs. Phosphorylated MORs are mostly internalized via clathrin-coated pits into early endosomes and subsequently dephosphorylated by intracellular protein phosphatases. The dephosphorylated MORs may either be recycled to the plasma membrane or transported to lysosomes for degradation. Previous biochemical studies on cultured enteric neurons have indicated that fentanyl induces either the functional desensitization or internalization of MORs (Minnis *et al.* 2003). In contrast, under the same condition, morphine does not promote the detectable internalization of MORs in cultured cells after prolonged or acute treatment in healthy animals, although it has been well-established that morphine causes the development of tolerance to its pharmacological actions (Minnis *et al.* 2003). On the other hand, recent studies have demonstrated that morphine activates MORs with promoting internalization of MORs via β-arrestin-2-dependent mechanisms in striatal neurons (Haberstock-Debic *et al.* 2005).

Thus, the mechanisms that underlie the development of analgesic tolerance to MOR agonists are very much complicated. To further understand properties of analgesic tolerance to MOR agonists, it has been necessary to investigate possible changes in analgesic efficacy following repeated treatment with MOR agonists at optimum doses just for the relief of chronic pain associated with physiological changes in the endogenous MOR system.

In a previous study, we demonstrated that repeated treatment with fentanyl caused a rapid desensitization to its ability to block hyperalgesia under an inflammatory pain state, whereas morphine did not have a similar effect (Imai *et al.* 2006). In addition, repeated treatment with fentanyl, but not morphine, resulted in the attenuation of MOR resensitization, and a subsequent increase in the levels of phosphorylated-MOR in the spinal cord of mice with inflammatory pain. These findings raise the possibility that chronic treatment with fentanyl may cause a different modulation of either the desensitization, internalization or resensitization of MORs in the spinal cord under a pain-like state compared with chronic treatment with morphine.

One mechanism for the MOR desnsitization or attenuation of MOR resensitization by fentanyl in the spinal cord under chronic pain could be a sustained increase in release of the endogenous μ-opioid neuropeptide β-endorphin after sciatic nerve ligation. In fact, it has been reported that β-endorphin is released within some brain regions during pain state (Zangen *et al.* 1998; Zubieta *et al.* 2001). In their reports, they mentioned that the extracellular levels of β-endorphin in the arcuate nucleus increased by 88% under pain-like state. Based on these findings, we assumed that β-endorphin might be released within the spinal cord, as well as brain regions, under pain-like state, as compensatory mechanism for the inhibition of pain transmisson. As sustained exposure to β-endorphin could results in receptor phosphorylation and uncoupling of receptors from effector systems, and thus desensitization, neuropathic pain associated with release of β-endorphin may interfere MOR resensitization by fentanyl.

To further understand the mechanisms that underlie the development of tolerance to this opioid analgesic-induced antihyperalgesic effect under chronic pain, we evaluated the effect of repeated administration of morphine, fentanyl or oxycodone on neuropathic pain-like hyperalgesia and the possible development of tolerance following sciatic nerve ligation. As in the mouse model of inflammatory pain, we demonstrated that repeated treatment with fentanyl, but not morphine or oxycodone, caused a rapid desensitization to its antihyperalgesic effect in nerve-ligated mice. Furthermore, we found that β-endorphin could be a key modulator for the high degree of antinociceptive tolerance to fentanyl caused by sciatic nerve injury. Based on this phenomenon, the present study was performed to investigate the effects of fentanyl on antihyperalgesic effect in β-endorphin knockout (KO) mice.

MATERIALS AND METHODS

The present study was conducted in accordance with the Guiding Principles for the Care and Use of Laboratory Animals of Hoshi University, as adopted by the Committee on Animal Research of Hoshi University. Every effort was made to minimize the numbers and any suffering of animals used in the following experiments.

Animals

Male and female β-endorphin derived from *proopiomelanocortin* (POMC) gene-KO mice (8–13 weeks old, 22–30 g) (The Jackson Laboratory, Bar Harbor, ME, USA), which had a C57BL/6J and 129S2/SvPas mixed genetic background as described previously (Niikura *et al.* 2008), their wild-type (WT) male and female C57BL/6J mice (8–13 weeks old, 22–30 g) (The Jackson Laboratory, Bar Harbor, ME, USA) and male ICR mice (7–9 weeks old, 20–25 g) (Tokyo Laboratory Animals Science Co., Ltd., Tokyo, Japan) were used in the present study. Animals were housed in a room maintained at 23 ± 1°C with a 12-hour light–dark cycle. Food and water were available *ad libitum*. Each animal was used only once.

Drugs

The drugs used in the present study were fentanyl citrate (Hisamitsu Pharmaceutical Co., Inc., Tokyo, Japan), morphine hydrochloride (Daiichi-Sankyo Co., Tokyo, Japan), oxycodone hydrochloride (a kind gift from Shionogi Pharmaceutical Co. Inc., Osaka, Japan) and β-endorphin (Sigma-Aldrich Co., St. Louis, MO, USA), which were dissolved in 0.9% physiological saline (Otsuka Pharmaceutical Co. Inc., Tokyo, Japan) for *in vivo* experiments or assay buffer for *in vitro* experiments.

Neuropathic pain model

Mice were anesthetized with 3% isoflurane. We produced a partial sciatic nerve injury by tying a tight ligature with a 8-0 silk suture around approximately one-third to one-half the diameter of the sciatic nerve on the right side (ipsilateral side) under a light microscope (SD30, Olympus, Tokyo, Japan), as described previously (Seltzer *et al.* 1990; Malmberg and Basbaum 1998). In sham-operated mice, the nerve was exposed without ligation.